

A novel feature-based probability of detection assessment and fusion approach for reliability evaluation of vibration-based diagnosis systems

Structural Health Monitoring

2020, Vol. 19(3) 649–660

© The Author(s) 2019

Article reuse guidelines:

sagepub.com/journals-permissions

DOI: 10.1177/1475921719856274

journals.sagepub.com/home/shm



Daniel Adofo Ameyaw , Sandra Rothe and Dirk Söffker

Abstract

Structural health monitoring systems are based on suitable sensor techniques allowing online and offline supervision of technical systems. The quantification of sensors/measurement devices is a key issue for qualifying their effectiveness and efficiency and therefore to ensure safe operations. Probability of detection serves as a performance measure for quantifying the reliability of conventional nondestructive testing procedures taking into account statistical variability of sensor-based measurements. For vibration-based supervision approaches and fault detection and isolation methods, the probability of detection approach cannot be applied similarly. This results mainly from the complexity of the dynamical behavior of systems monitored in relation to faults, sensors position (observability), and the related feature extraction or monitoring task. In this contribution, probability of detection evaluation of vibration-based fault detection of elastic mechanical structures to be monitored is developed. Beside a principal discussion of the problem serving as introduction, an example using different sensor types in combination with mechanical modifications of an elastic beam is presented. The $\alpha_{90/95}$ -criteria representing probability of 90% detection at a confidence level of 95% is examined to the measurements and related outcomes. Based on the analysis of a suitably chosen feature (like eigenfrequency or band power) and dependent on the mechanical modes considered, the efficiency and deficiency of the different combinations are shown. Based on the proposed approach, a new insight into the usefulness of different sensor type and fault position combination becomes possible. To improve the detection quality, suitable assumptions in combination with sensor/information fusion are applied to feature-based analysis as detection task using vibration measurements. In addition, based on an experimental evaluation, it can be concluded that a suitable fault-feature probability of detection analysis can be successfully implemented as a new reliable measure for vibration-based fault detection and isolation approaches. Furthermore, decision fusion as the combination of different measurements will allow the improvement of results. Dependent on noise analysis, a trade-off between flaw size detection and probability of falsely characterizing a fault with $\alpha_{90/95}$ reliability level can be attained.

Keywords

Probability of detection, fault detection and isolation, structural health monitoring, vibration analysis, fault diagnosis, multi-sensor, reliability evaluation

Introduction

The presence of defects in systems/components may affect its structural and functional integrity. From this, it can be concluded that the structural/functional integrity as well as the quality of detection and diagnosis approaches are connected. In the last decades, several fault detection and isolation (FDI) techniques are implemented to detect changes, faults, and local defects. These methods can be grouped into four categories: signal-based, model-based, data-driven, and hybrid approaches. Signal-based approaches utilize output

signals. Here, fault detection modules often compare raw or filtered signals to thresholds and conclude the presence of faults. Faults are defined as the occurrence of unacceptable changes to given healthy measures, indicators, and other suitable characteristics describing

Universitat Duisburg-Essen, Duisburg, Germany

Corresponding author:

Daniel Adofo Ameyaw, University of Duisburg-Essen, Lotharstrasse 1-21, Duisburg 47057, Germany.

Email: daniel.adofo-ameyaw@uni-due.de

the regular status of the system monitored. Model-based approaches use, beside output signals, input signals and requires a model to be built (parameter identification), to be assumed (observer), or to be suitably established.^{1,2} Data-driven approaches formulate implicit relationships by trained models through analysis of fault-free data obtained during regular operations.² These models are used to estimate the behavior of variables to be compared to those obtained from measurements.³ Hybrid approaches combine model-based and model-free techniques.⁴

Signal-based methods are widely adopted. The main idea is to extract relevant process characteristics from analyzed sensor data and combine this with further knowledge (clearly related to specific health states of the system).⁵ Condition-monitoring frameworks involve data acquisition and normalization, feature extraction, and, if required, the development of statistical models. Feature extraction is performed in time, frequency, and time–frequency domain transforming a measured signal to a new representative form to make classification tasks easier, or more reliable.

Classification-related performance indices (PI) are important to evaluate FDI approaches. For this, related measures like detection rate (DR) or false alarm rate (FAR) are evaluated based on the confusion matrix. When discussing the effects of varying tuning parameters, the complete precision values of the receiver operating characteristic curve (ROC) can be used for evaluation.⁶ Typical evaluation considers a single set of numbers describing also the uncertainty of statements. Fault tolerant control systems apply FDI techniques and reconfigure controllers to enhance the entire system reliability.^{7,8} Reliability evaluation of FDI schemes itself still remains an open problem.

Structural health monitoring (SHM) is the process of implementing a damage detection and characterization strategy for monitoring engineering structures.^{9,10} Damage in this context describes physical changes that adversely affects the system performance.¹⁰ The field of SHM increasingly has become an essential aspect of industrial practice to ensure the quality of products, safe operations, improved maintenance, and to save cost. Many engineering structures are approaching or exceeding their initial design life, making SHM relevant.¹¹ In SHM, monitoring is mainly applied online for large structures.¹⁰ Nondestructive testing (NDT) in contrast is usually applied offline after damage localization, though it is used for in situ monitoring of structures like pressure vessels, rails, aircraft components, among others. Safety-critical and high capital expenditure elastic structures have a wide application range in mechanical, civil, and aerospace fields. These include structures like turbomachinery, blades and towers of wind turbines, aircraft fuselages, bridges, skyscrapers,

among others. These systems are susceptible to changes caused by material specific properties like cracks (in metals, fibers etc.) or delamination (composites). Vibration monitoring of these elastic structures is common in industrial practice. Vibration-based SHM operates on the principle that structural defects result in changes in dynamical properties. Fault identification is mainly based on displacement, velocity, or acceleration measurements at a single point;¹² however, useful assessments may include observable effects and multi-point measurements. It should be noted that the evolution of the damage and changes in the dynamics of the structure act on different time scales.¹² The evolution of the damage is slower compared to the vibration of the structure, except for impact damage. Despite the advances in SHM, questions remain. These include the transition from theory to practical implementation, early detection of faults, and reliability assessment of diagnostic statements.^{1,9} The dynamics of vibrating systems changes due to different effects like altering of the structure possibly leading to changes in the mass, stiffness, and damping properties. Finally, decisions about the existence of changes (fault detection) and/or specific faults (diagnosis) have to be made. Making reliable decisions is of importance. Current FDI approaches utilize classification-related performance measures. These performance measures are subject to uncertainties; hence, the reliability is not quantified. Conversely, conventional NDT approaches use the probability of detection (POD) concept as a reliability measure. The emergence of SHM led analysts to ponder how to integrate POD in SHM systems. In comparison to NDT, SHM systems are mounted permanently and should provide reproducible results. Aging of the structure leads to adverse effects. In Aldrin et al.,¹³ Monte Carlo simulation of flaw size as a function of time is proposed. The results demonstrate the sensitivity of flaws to degradation of SHM system. In NDT, uncertainties are associated with human factors, variations in the interface between the structure and transducer, crack form and shape, and local structure properties, while SHM uncertainties are environmental conditions, aging effects in the structure, and damage morphology.¹⁴ In Mendrok and Uhl,¹⁵ experiments are undertaken on an aluminum frame to ascertain the POD capabilities of a modal filter-based damage detection SHM system. Ten accelerometers are mounted on various positions on the frame. An impulse test is carried on the specimen and the obtained damage index values and the corresponding damage sizes are the input data to determine POD curve. However, individual sensor-POD characterization is neglected. Also, variations in fault position and the effect on the POD curve are not considered. Model-assisted POD is proposed in Aldrin et al.¹⁶ and Mueller et al.¹⁷ utilizing numerical models; however,

numerical efforts and computational time problems have to be solved for convenient applications in practice. Also, the ability of these models to simulate real faults remains as open tasks. The POD approach typically quantifies a sensor/filtering technique in combination with mostly static measurements. Implementing this measure in the field of vibration-based SHM is difficult. Difficulties result from the complexity of dynamical behavior in relation to faults, sensors position (observability), related data analysis procedures, and the system under consideration. The POD approach usually uses a so-called POD curve, constructed by plotting the accrual of flaws detected against the flaw size or produce a response over a threshold.^{18,19} The POD theory as required is briefly repeated in the next section.

This contribution extends the first results and ideas of the authors published in Ameyaw et al.^{20,21} In addition to these publications, in this article, the theory of the new approach is completely developed, the results presented are extended, and a new discussion regarding different combination approaches, POD view to FDI, and POD-based noise analysis of fault diagnosis systems is added. The fusion approach establishes clearly the theory and considers all sensors in the combination process. The POD view to fault diagnosis discusses in detail the detection task and quantification metric for reliability evaluation of sensors. Noise analysis based on POD is introduced in this work to determine FAR for a selected sensor threshold. The article is organized as follows: a brief theory of the POD measure is introduced. This is followed by explaining the experimental setup required for illustration of the effects. Results and a new approach to fuse POD values are given. A POD view to fault diagnosis is presented, followed by a POD perspective to noise analysis and finally the conclusion.

POD

According to previous studies,^{14,18,19} the POD approach allows a general assessment of the reliability of NDT methods and lately SHM systems. The aim of the $a_{90/95}$ criteria is to specify a damage size, which can be detected/missed applying a specific method to be evaluated, taking into account statistical variability of the sensor and measurement properties. The United States Air Force (USAF), National Aeronautics and Space Administration (NASA), as well as many authors consider MIL-HDBK-1823A (updated version of MIL-HDBK-1823) as the state-of-the-art and contemporary guide for POD studies.^{22,23} This article adapts the method and utilizes extracted features as response. It is worth mentioning that this research focuses on fault detection. Here, classical sensors in

combination with a vibration-oriented system response analysis are utilized. Difficulties associated with observable effects, faults and sensor positions, and the non-uniqueness of the POD curve characteristics for which not so much attention is given in literature with respect to these combinations are demonstrated. Data used in producing POD curves are categorized by the main variables to be combined in the POD approach. These data are the following:

1. Hit/miss: produce binary statement or qualitative information about the existence of a flaw.
2. Flaw size versus response (a vs \hat{a}): systems which also provide some quantitative measure of size of target.

A typical and useful criteria for detection at a 90% POD level with 95% confidence level is the so-called flaw size detectability. In the derivation of the POD curve, first, a regression analysis of the data gathered has to be realized.^{19,24,25} Let $x = f(a)$ and $y = f(\hat{a})$, the regression equation for a line of best fit to a given data set is given by

$$y = b + mx \quad (1)$$

where m is the slope and b the intercept. Here, the 95% Wald confidence bounds on y is constructed by

$$y_{(a=0.95)} = y + 1.645\tau_y \quad (2)$$

where 1.645 is z -score of 0.95 for a one-tailed standard normal distribution and τ_y the standard deviation of the regression line. The delta method is a statistical technique used to transition from regression line to POD curve.¹⁹ The confidence bounds are computed using the covariance matrix for the mean and standard deviation POD parameters μ and σ , respectively. To estimate the entries, the covariance matrix for parameters and distribution around the regression line needs to be determined. This is done using the Fisher's information matrix I . The information matrix is derived by computing the maximum likelihood function f of the standardized deviation z of the regression line values. The entries of the information matrix are calculated by the partial differential of the logarithm of the function f using the parameters of $\Theta(m, b, \tau)$ of the regression line.

From

$$z = \frac{(y - (b + mx))}{\tau} \quad (3)$$

and

$$f = \prod_{i=1}^n \frac{1}{2\pi} e^{-\frac{1}{2}(z)^2} \quad (4)$$

the information matrix I can be computed as

$$I_{ij} = -E\left(\frac{\partial}{\partial \Theta_i \partial \Theta_j} \log(f)\right) \quad (5)$$

The inverse of the information matrix yields ϕ as

$$\phi = I^{-1} = \begin{bmatrix} \sigma_b^2 & \sigma_b \sigma_m & \sigma_b \sigma_\tau \\ \sigma_m \sigma_b & \sigma_m^2 & \sigma_m \sigma_\tau \\ \sigma_\tau \sigma_b & \sigma_\tau \sigma_m & \sigma_\tau^2 \end{bmatrix} \quad (6)$$

The mean μ and standard deviation σ of the POD curve are calculated by $\mu = (c - b)/m$, where c is the decision threshold and $\sigma = \tau/m$. The cumulative distribution Φ is calculated as

$$\Phi = \frac{1}{2} \left[1 + \operatorname{erf} \frac{x - \mu}{\sqrt{2}\sigma} \right] \quad (7)$$

The POD function is derived as

$$POD(a) = \Phi \left[\frac{a - \mu}{\sigma} \right] \quad (8)$$

Using this formula, the POD curve can be set up for varying flaw sizes.

Adaptation and application of POD in vibration-based fault diagnosis

The idea of this article is to adapt standard POD measurement and implementation strategy to vibration-based health monitoring and therefore integrate vibration analysis results (as shown in Figure 1).

Conventional NDT approaches apply statistical analysis and show the relationship between signal strength \hat{a} and the size a of the flaw initially causing measurements. The time and cost involved in POD analysis have given rise to model-assisted POD (MAPOD) to improve the effectiveness of POD models with little or no specimen testing by utilizing model-generated data.²⁶ Two MAPOD methods exist.²⁷ The transfer function approach is a physics-based method that transfers the computed POD curve for a specific process to another with different parameters.²⁸ The second method utilizes physics-based models to propagate directly the uncertainty of a given set of assessment/examination parameters. The idea of this article is to discuss fault diagnostics from a POD-oriented view. Experiments have to be carried out including variations of faults (denoted by a) to ascertain the influence of faults on the observed value. The observed value is thus an aggregation of the signature of the system and fault.

Since SHM systems are permanently mounted, data are continuously recorded. Through signal processing, suitable features (e.g. eigenfrequencies and band power) are extracted from time series data. The feature extraction task reduces noise effects. Uncertainty in measured data is accounted by constructing prediction bounds. The prediction bounds ensure that for every new 100 observations, 95 of them should fall within the bounds. Currently, classification approaches are used in monitoring vibrating systems (illustrated in Figure 1) but incapable of quantifying vibration-based fault measurements. However, the POD measure from the NDT and material testing field can be effectively implemented in

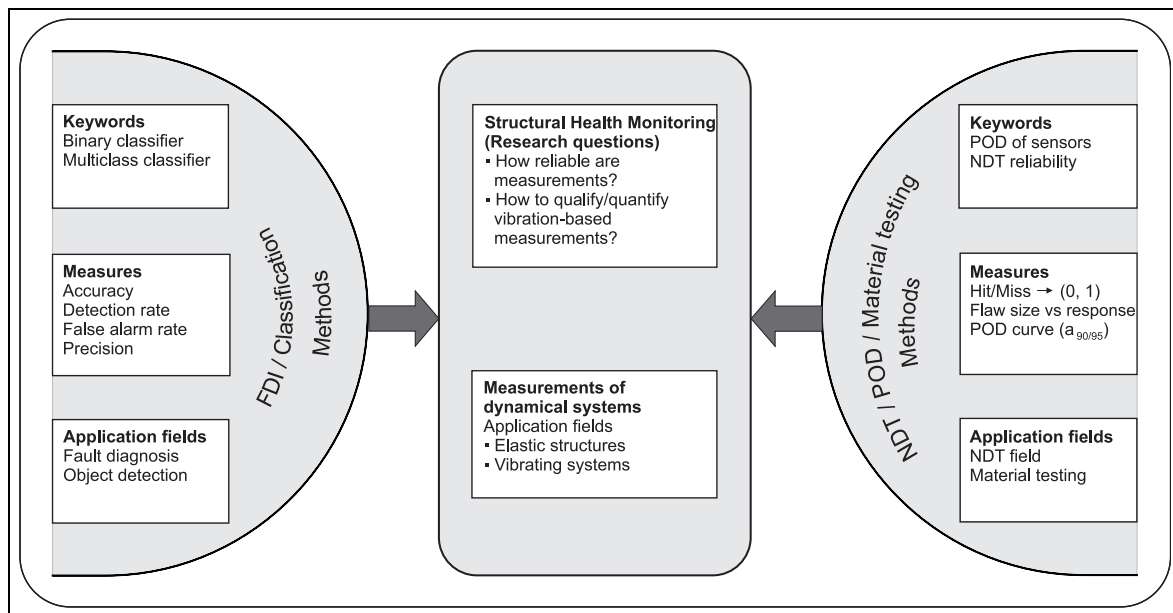


Figure 1. General idea.

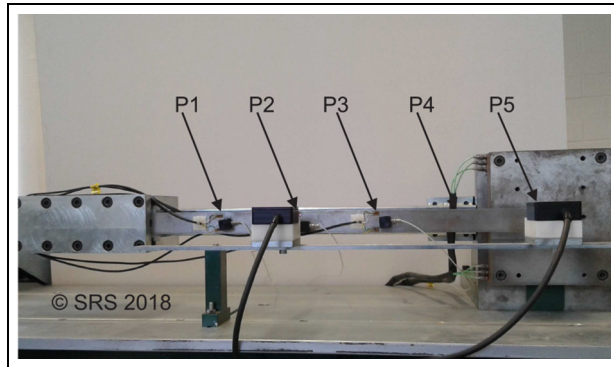


Figure 2. Test rig (Chair SRS, UDuE) consisting of a one side clamped elastic beam with bonded strain gauges, laser sensors, and accelerometers.

vibration-based fault diagnosis to quantify sensor-related measurements and therefore be used alongside known classification approaches.

Experimental results

Using a simple benchmark test rig, the principal problem associated with implementation of POD in vibration-based SHM is demonstrated. The experimental system to be considered for illustration is an elastic beam. Acceleration, displacement, and strain measurements are taken. As features, band power and eigenfrequency analysis are carried out on the first two modes of the mechanical system. The obtained results and the analysis are discussed in detail.

Experimental setup

The experiment is carried out on an elastic mechanical beam using the test rig in Figure 2. An elastic steel beam of dimensions $545 \times 30 \times 5$ mm is clamped on one side. The beam length is divided into five equal parts (Figure 3) defining sensors position. Piezoelectric accelerometers are attached at three positions (P1, P2, and P3) on the beam. Two strain gauges are bonded onto the beam at positions P1 and P3. Two displacement measurements are taken at the two positions (P2, P4) using noncontact laser sensors. The beam can be excited manually or by modal hammer.

Injected faults as changes to be investigated

In this article, changes within the elastic mechanical structures are assumed as changes due to varying mass, so here additive masses are applied to modify the existing initial system to simulate a fault (due to mass change). Two cases of point mass placement are examined. Case I involves placing the point mass at midpoint

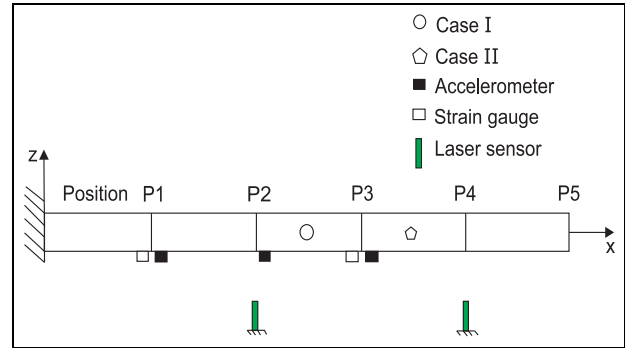


Figure 3. Sensor positions relative to beam length.

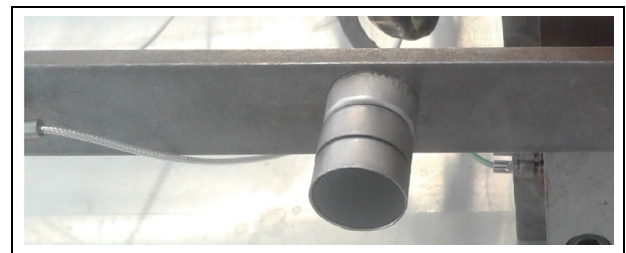


Figure 4. Mechanical beam modification using additive mass.

of positions 2 and 3. Case II involves the placement of point mass at the midpoint of positions 3 and 4. These masses are added to the specified locations. For every incrementally placed mass (Figure 4), the beam is excited and the corresponding data are recorded.

Results

The analysis is carried out for the first and second mode for each situation of mass placement (cases I and II). In Figure 5, time series data for different sensors used in the experiment are given. The regression analysis, confidence bounds, prediction bounds, and the POD characterization for each sensor are carried out. The strategy to map the data to the POD curve is shown (Figure 6). In Figure 6, a graphical representation of the flaw size versus response approach elaborated earlier is given. It involves setting threshold values and fitting trendline to the data. Confidence and prediction bounds are constructed on both sides of the line of best fit. Probability density functions at each flaw size are established. The area above the decision threshold is used to construct the POD curve.

It should be stressed that the focus of the work is on fault diagnosis and not on classical material testing approaches. The results are given in Table 1. From the results, it becomes evident that the $a_{90/95}$ POD

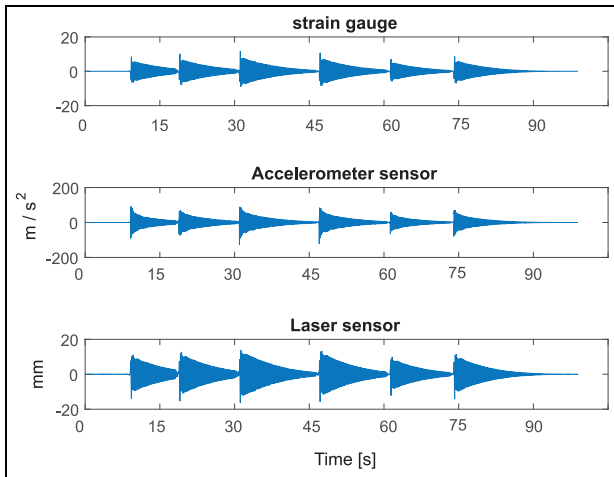


Figure 5. Signals of different sensors.

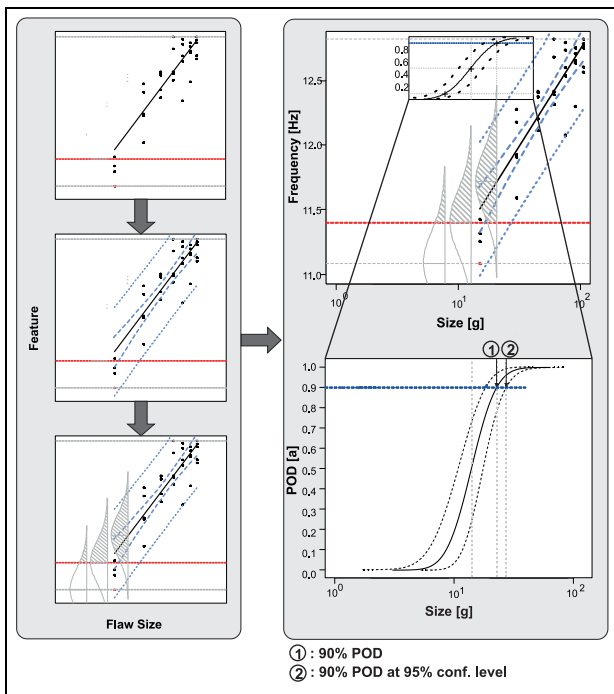


Figure 6. Strategy from data to POD curve.

quantification is different depending on sensor type and mode considered. Based on fault position, sensor location relative to fault, sensor type, and the mode considered, different results are obtained. The numbers indicate the maximum mass that can be missed with a 90% POD at a 95% confidence level. The lowest masses (^a) represent best results, so the sensor detects least mass change. The worst (^b) POD sensor characterization represents worst results so the sensor requires large fault (here: mass) values to be detected with $a_{90/95}$ reliability. To explore the nonuniqueness of a feature

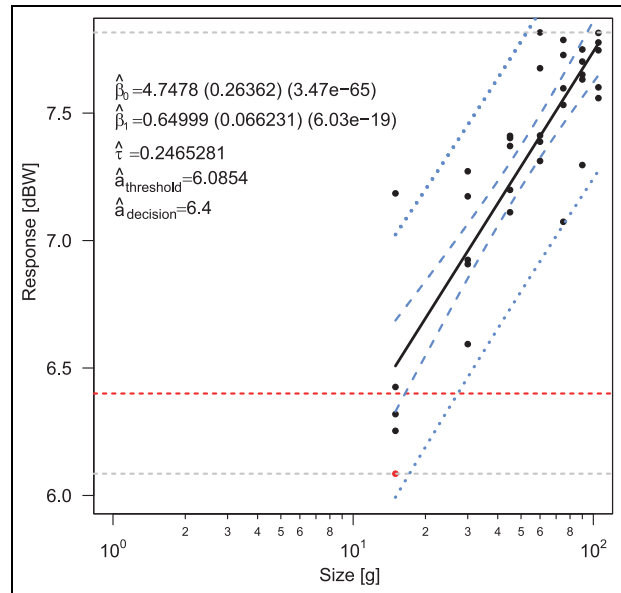


Figure 7. Regression analysis related to band power.

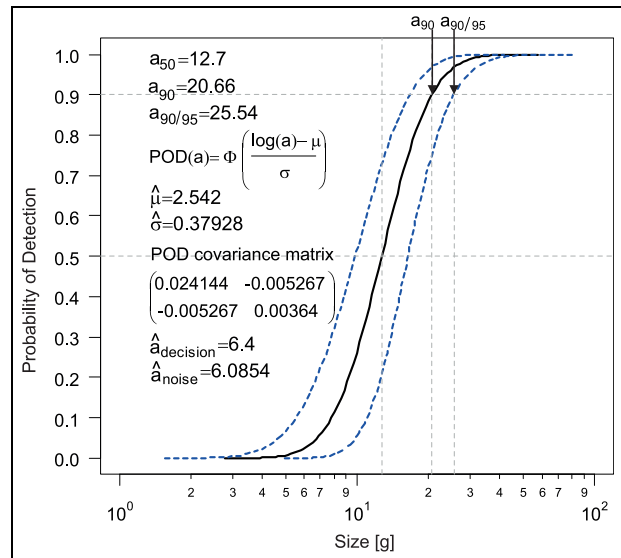


Figure 8. POD related to band power feature.

for POD analysis, as additional feature, band power is also extracted. The band power (here: 0-500 Hz) represents the average power utilizing the Euclidean norm. Analysis for this feature is given in Figures 7 and 8. The results are compared with the eigenfrequency results (Table 1).

It can be concluded that the POD of vibration-based analysis of elastic structures strongly depends on sensor type (dynamic range differs for each sensor), sensor position (same sensor at different positions produce different results), fault position (case I or II), and attribute

Table 1. Measure: Eigen frequencies (modes 1 and 2) and band power.

Sensor	Point mass between P2 and P3 (case I)			Point mass between P3 and P4 (case II)		
	Mode 1 $a_{90/95}$ POD (g)	Mode 2 $a_{90/95}$ POD (g)	Band power $a_{90/95}$ POD (g)	Mode 1 $a_{90/95}$ POD (g)	Mode 2 $a_{90/95}$ POD (g)	Band power $a_{90/95}$ POD (g)
ACC 1 at P1	74.04	48.15 ^a	45.28 ^b	52.21	9.915	84.56 ^b
ACC 2 at P2	74.04	55.78	34.63	52.15	9.293 ^a	22.78
ACC 3 at P3	74.04	72.59 ^b	20.20 ^a	52.15	13.36	17.29 ^a
SG 1 at P1	85.19	72.38	29.34	52.15	11.07	28.69
SG 2 at P3	126.70 ^b	62.23	34.37	54.08 ^b	9.394	27.93
Laser 1 at P1	67.30 ^a	61.03	27.64	52.10 ^a	43.49 ^b	25.54
Laser 2 at P4	74.04	–	23.44	52.15	–	25.85

ACC: accelerometer; P: position; POD: probability of detection; SG: strain gauge.

^aBest results.

^bWorst results.

selected (eigenfrequency or band power). Consequently, it can be stated that general statements about the usefulness of related sensors are not possible. Depending on effects, measurement options, features considered, and sensor type, the choice becomes sophisticated and task-specific.

Fusion of results to combine individual FDI-statements

In the case of nonreliable statements (the use of one sensor and feature is not suitable to ensure confident health status statements), decision fusion of the results from different sensors or features may be an option for improving reliability. This section details a new approach used to improve the POD characterization of each sensor-/vibration-based statement by decision fusion using several sensors. To fuse the detection results of the sensors related to their POD and $a_{90/95}$ value, the Bayesian Combination Rule (BCR) can be applied. The BCR also known as Bayes belief integration or Bayesian belief method is a well-known and commonly used fusion technique based on conditional probability.

To set up the conditional probabilities of each classifier for each class, first, the confusion matrix has to be calculated. The confusion matrix C^k for each classifier e_k with $k = 1, \dots, K$, where K is the total number of considered classifiers, is defined as

$$C^k = \begin{bmatrix} C_{11} & C_{12} & \dots & C_{1M} \\ C_{21} & C_{22} & \dots & C_{2M} \\ \vdots & \vdots & \ddots & \vdots \\ C_{M1} & C_{M2} & \dots & C_{MM} \end{bmatrix} \quad (9)$$

where $i, j = 1, \dots, M$ with M as the number of classes. The element C_{ij} is the number of samples, where the

classifier e_k has assigned class j and the actual class of the sample is i .

Using the elements of the confusion matrix, the probability that sample x belongs to class i , if the classifier e_k assigns x to class j , can be calculated using

$$P_{ij} = P(x \in i | e_k(x) = j) = \frac{C_{ij}^k}{\sum_{i=1}^M C_{ij}^k} \quad (10)$$

For each classifier e_k , the probability matrix P^k is set with

$$P^k = \begin{bmatrix} P_{11} & P_{12} & \dots & P_{1M} \\ P_{21} & P_{22} & \dots & P_{2M} \\ \vdots & \vdots & \ddots & \vdots \\ P_{M1} & P_{M2} & \dots & P_{MM} \end{bmatrix} \quad (11)$$

The diagonal values ($i = j$) are the same as the precision value for this class. Based on the probability matrix of each classifier, a combined belief value $bel(i)$ for each class i is determined for each sample with the formula

$$bel(i) = \frac{\prod_{k=1}^K P_{ij_k}}{\sum_{i=1}^M \prod_{k=1}^K P_{ij_k}} \quad (12)$$

where j_k is the assigned class of classifier e_k for the considered sample x . The maximum of the belief values is used to make a decision for one of the classes.

In the case of fault detection, normally the precision value is used as a performance measure, which is considered in the fusion process. Here, the measurable POD values for specific masses are assumed as replaceable for the precision value, because both define a performance measure about the reliability of an

Table 2. POD results for case I—band power feature.

Sensor	POD (20.20 g)	POD (23.44 g)	POD (27.64 g)	POD (29.34 g)	POD (34.37 g)	POD (34.63 g)	POD (45.28 g)
ACC 1	48.6	61.8	71.6	74.0	83.9	84.8	90.0
ACC 2	63.5	71.2	83.2	84.8	89.7	90.0	96.1
ACC 3	90.0	95.0	97.1	97.6	98.8	98.9	99.5
SG 1	74.5	83.9	85.8	90.0	94.4	94.7	95.8
SG 2	64.2	75.5	84.3	85.7	90.0	91.1	96.0
Laser 1	77.7	87.1	90.0	91.6	94.5	95.4	98.1
Laser 2	85.5	90.0	93.7	95.3	97.2	98.1	99.2

ACC: accelerometer; POD: probability of detection; SG: strain gauge.

assignment. Therefore, the POD of each sensor and feature for specific faults (here: masses denoted as $a_{90/95}$ values for the considered sensor–feature combination) can be used to calculate the belief values according to the BCR. In Table 2, the POD of the seven sensors for the corresponding $a_{90/95}$ values is given. To explain the combination using POD values, the fusion of the sensors ACC 1 and ACC 2 is considered as example. To calculate the belief values, it has to be known which sensor detected the fault and which failed. Assuming ACC 1 detected a fault, ACC 2 did not, the values used for belief value calculation are denoted as $P_1 = POD_{20.20g}^{ACC1}$ and $P_2 = POD_{20.20g}^{ACC2}$. The belief value for the mass of 20.20 g is calculated by

$$bel(20.20g) = \frac{P_1 \cdot (1 - P_2)}{P_1 \cdot (1 - P_2) + (1 - P_1) \cdot P_2} \quad (13)$$

In the same way, the belief values for the other masses can be calculated. Extending the fusion to all sensors, the number of detection combinations ascends.

The resulting belief values for different detection combinations, as example if five of the seven sensors detected a fault (e.g. 0 0 1 1 1 1 1 means the first two sensors (ACC 1 and ACC 2) did not detect a fault, all other did), are shown in Figure 9. Depending on which five of the seven sensors detect the fault, the belief values vary. Although, all belief values increase for increasing masses. This means that the probability that a fault with a higher mass is present is higher in case of five sensors detecting a fault. In Figure 10, a selection of different detection combinations is presented. For selection of the best and worst sensor-/feature-based statement, results according to Table 2 are considered. For example, 4B means the four best sensors have detected a fault, the others did not. In case of 6B, 5B, and 4B, all belief values are close to 100%, while in case of 1W, 2W, and 3W, all belief values are close to 0% (see Figure 10). For the other cases, a symmetry can be seen, for example, the curve of 5W corresponds to 100% minus the curve of 2B.

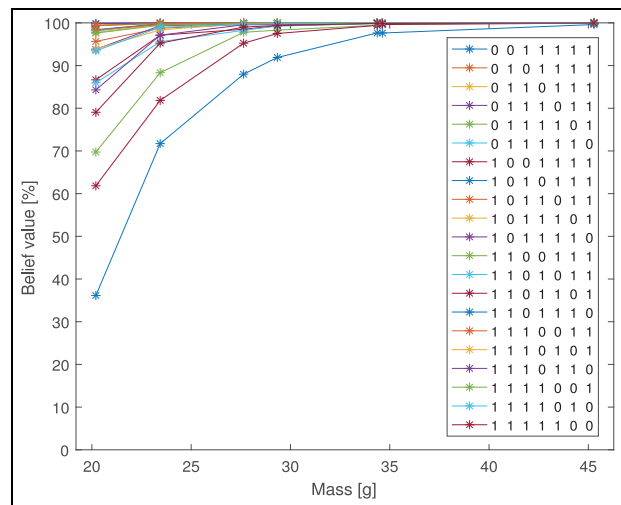


Figure 9. Belief values for different detection combinations, when five of seven sensors detect a fault.

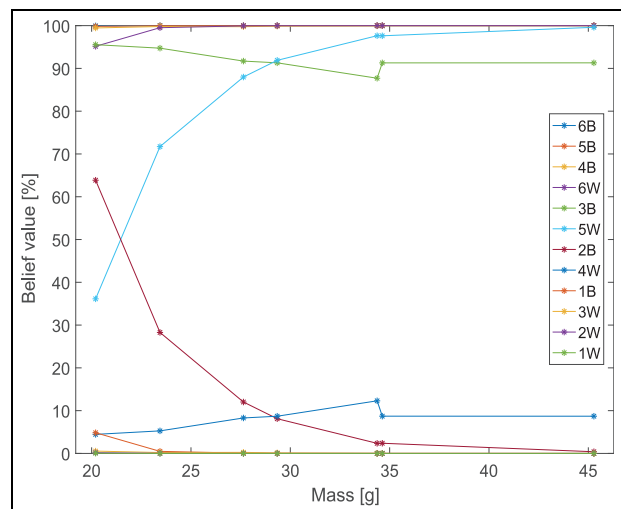


Figure 10. Belief values for different detection combinations, selected by the best (B) or worst (W) sensors detecting the fault.

Considering the case 2B, which means the two best sensor-/feature-based statement (with the lowest $a_{90/95}$ value) are detecting a fault, all other five sensors are not, it is more probable that there is a small fault than a bigger one, because if the better sensor-/feature-based statement has detected a fault, it could be that the fault is too small to be detected by the other sensors (with higher $a_{90/95}$ value). However, if the mass would be larger, the other sensors should also have detected the fault. If there is a higher number of sensors detecting a fault (like in case 5W), the belief values increase for increasing masses, because a larger fault is easier to detect.

Using the introduced fusion approach, the probability of the presence of a specific mass (as fault) can be obtained based on the individual performance and assignments of the sensor-/feature-based statement.

POD view to FDI

SHM systems applied to vibrating elastic structures usually denote monitoring dynamical systems. Arising questions are related to the reliability of measurements. Consequently, this also affects related diagnostics statements about diagnosis and therefore strongly affects the reliability of vibration-based measurements. The POD-strategy introduced now allows the quantification of vibration-based measurements (here: fault size). Further, a new adaption of POD measure is proposed and implemented with respect to the integration of the vibration analysis. Conventional NDT approaches apply statistical analysis and use the relationship between signal strength \hat{a} and the size a of the target initially causing the measurement. The variation of this can be discussed from a FDI-oriented view. In SHM, additional data analysis is required to convey information about the signal's attributes. The response is a feature-based response. The output sensor values for varied fault size have to be recorded. Through signal processing, suitable features have to be extracted and used as response. Four possible graphs (a vs \hat{a} , a vs $\log(\hat{a})$, $\log a$ vs \hat{a} , $\log a$ vs $\log \hat{a}$) have to be plotted. The graph with best linearity, uniform variance, and uncorrelated observations is selected.

The detection task corresponds to the response threshold value ε . This can be obtained from the regression line, confidence bounds, and 90% probability density (Figure 11). From the general equation of the confidence bounds equation (2), the values of slope, gradient, and standard deviation can be measured directly from the regression line. However, the size a generating $a_{90/95}$ value can be obtained from the regression line in combination with the POD curve as indicated in Figure 11. The threshold ε defines the response

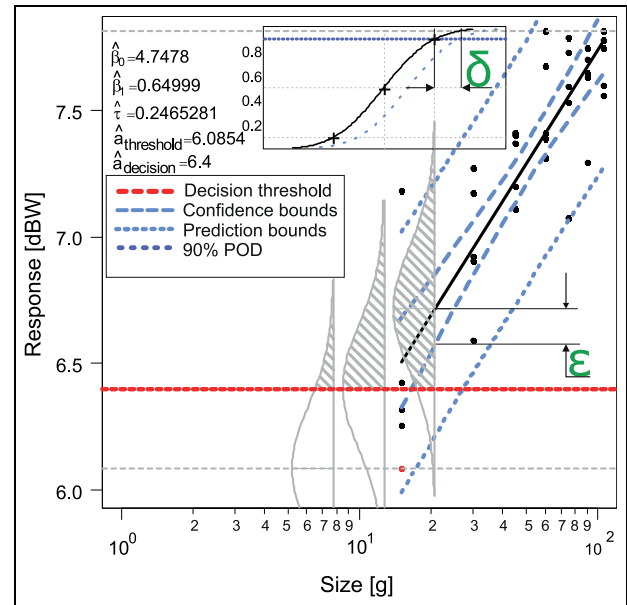


Figure 11. Detection task.

detection value, beyond which the fault can be detected with a $a_{90/95}$ reliability. The $a_{90/95}$ value δ quantifies the threshold size. The threshold ε permits reliability certification of the response value for a specific sensor and the subsequent quantification of the response in terms of fault size. The results for this example indicate that a response of 0.14 dBW is the threshold value ε , which corresponds to a fault size δ of 4.88 g. From the demonstrated consideration, it can be stated that this is a new and significant insight for task-/application-specific quantification of sensors and serves as detection and quantification metric for reliability evaluation of sensors. This new view to a classical problem as well as classical solutions should improve monitoring/fault detection system designers to learn about the complexity of the problem and therefore to improve detection systems by choosing the right combination of task, sensor, feature, and sensor position.

Noise analysis-based discussion

The observed signal is an aggregation of the characteristics of the system to be considered combining signatures, errors, and noise effects. Classical POD methods usually evaluate independently the healthy state or infer noise from data not associated with target size.^{19,24} This article, however, incorporates both approaches by measuring the healthy and defective states. Both states are combined/plotted, and the effect of the selected response decision threshold (y_{th}) on the probability of false positive (PFP) for a specific sensor is inferred from the noisy data. Noise here refers to healthy state data

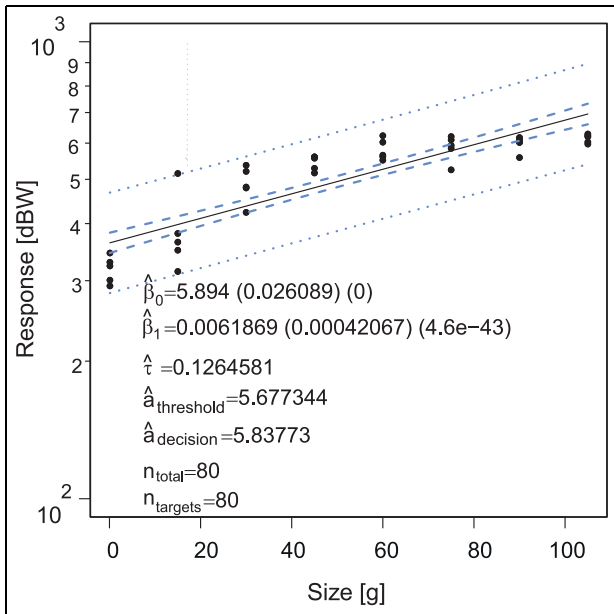


Figure 12. Accelerometer at position 2 band power data.

since it is not related to flaw size. To illustrate this relations here as example, accelerometer-based measurements at position 2 filtered as band power (Figure 12) are used.

A χ^2 (chi-square) test is undertaken to identify the nature of noise distribution. Various distributions are tested, with the Gaussian distribution emerging most plausible. The χ^2 produced a p-value of 0.94, thereby rejecting the null-hypothesis that the distribution is non-Gaussian. A regression analysis is carried out on the noisy data and the mean μ_{noise} and standard deviation σ_{noise} are calculated (Figure 13). The PFP is the percentage of healthy data that the system classifies as damage. For a Gaussian noise distribution, the PFP is computed as

$$PFP = \int_{y_{th}}^{\infty} \frac{1}{\sqrt{2\pi}\hat{\sigma}_{noise}} e^{-\frac{(y-\hat{\mu}_{noise})^2}{2\hat{\sigma}_{noise}^2}} dy$$

The distribution with regard to PFP is illustrated in Figure 14 (shaded red area relative to the selected decision threshold).

Trade-off between PFP and POD

Using (as example) the accelerometer-based measurements at position 2 filtered as band power data (Figure 12) and assuming the sensors decision threshold (0) based on assumed Gaussian distribution, the point (1) results, denoting with (2) a related PFP. Assuming as threshold the $a_{90/95}$ criteria, the point (3)

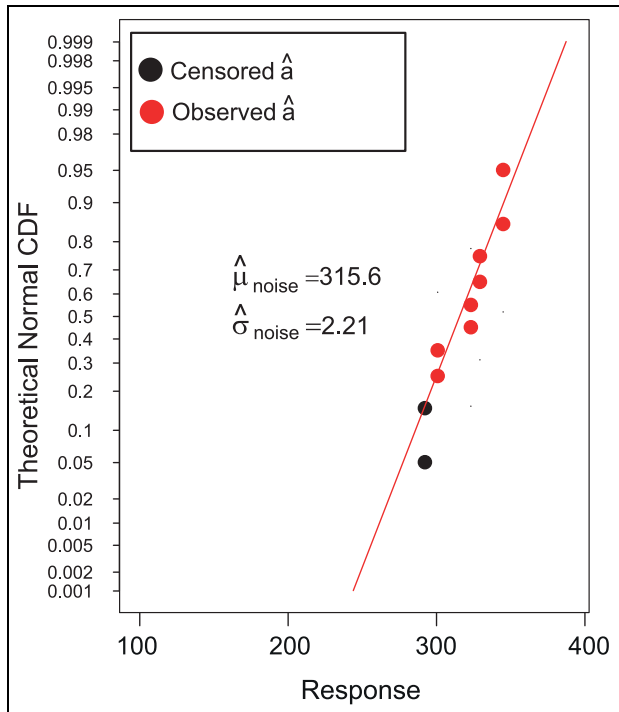


Figure 13. Noise analysis.

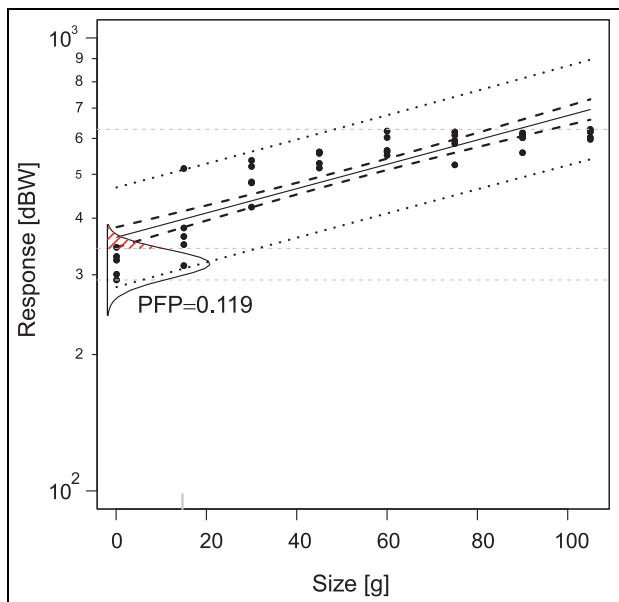


Figure 14. PFP for a specific decision threshold.

results, denoting with (4) a related maximum fault size to be missed. Figure 15 (as example) shows that based on the sensor property, the decision value can be obtained, here $\hat{a} = 343$. From the distribution, the character of the noisy data can be obtained. Assuming Gaussian distribution, the point (1) can be obtained, denoting number (2) with a resulting PFP of 0.12.

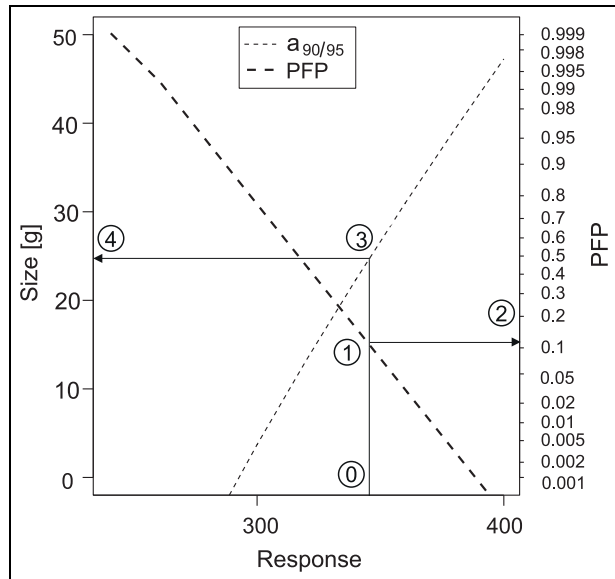


Figure 15. Tradeoff between flaw size, decision threshold, and PFP.

Assuming the $a_{90/95}$ criteria, the point (3) is defined so the maximum fault size to miss (here: 24.68 g) can be obtained.

Changing the sensor includes changing the distribution character (here: Gaussian) and the decision threshold. Other sensors will result in different distribution characters and different values. The character of the introduced strategy remains. Changing the assumption (here: relevant criteria $a_{90/95}$), a different value for the connection between the $a_{90/95}$ criteria and the obtained Gaussian characteristic (point 3) results, so that the fault size (4) is always affected.

Summary and conclusion

This article focuses on introducing a novel POD-oriented view to vibration-based diagnosis typically using sensor types. The measurements used are acceleration, strain, and displacement (laser sensors). The results indicate that the POD characterization depends on the sensor position, fault position, and the feature selected. The sensor type has an effect on the POD due to the fact that performance specifications vary for different sensors. The $a_{90/95}$ criteria representing probability of 90% at a confidence level of 95% is successfully implemented in vibration-based FDI as a reliability measure. The new insight introduced allows task-/application-specific quantification of sensors relative to vibration-based monitoring/diagnosis of faults. Using the novel fusion approach introduced, the probability

of the existence of a fault can be obtained based on the individual performance and assignments of the sensor-/feature-based statement. Noise analysis allows a decision threshold to be selected which permits a suitable trade-off between the POD and PFP.


Declaration of conflicting interests

The author(s) declared no potential conflicts of interest with respect to the research, authorship, and/or publication of this article.

Funding

The author(s) disclosed receipt of the following financial support for the research, authorship, and/or publication of this article: This work is partly supported by Deutscher Akademischer Austauschdienst (DAAD) through a PhD fellowship for the first author performing his PhD at the Chair of Dynamics and Control, U DuE, Germany.

ORCID iD

Daniel Adofo Ameyaw  <https://orcid.org/0000-0001-8035-7154>

References

1. Söffker D, Wei C, Wolff S, et al. Detection of rotor cracks: comparison of an old model-based approach with a new signal-based approach. *Nonlinear Dynam* 2016; 83(3): 1153–1170.
2. Isermann R and Balle P. Trends in the application of model-based fault detection and diagnosis of technical processes. *Control Eng Pract* 1997; 5(5): 709–719.
3. Ma J and Jiang J. Applications of fault detection and diagnosis methods in nuclear power plants: a review. *Prog Nucl Energ* 2011; 53(3): 255–266.
4. Poon J, Jain P, Konstantakopoulos IC, et al. Model-based fault detection and identification for switching power converters. *IEEE T Power Electr* 2017; 32(2): 1419–1430.
5. Al-Shrouf L, Saadawia MS and Söffker D. Improved process monitoring and supervision based on a reliable multi-stage feature-based pattern recognition technique. *Inform Sciences* 2014; 259: 282–294.
6. Widodo A and Yang BS. Support vector machine in machine condition monitoring and fault diagnosis. *Mech Syst Signal Pr* 2007; 21(6): 2560–2574.
7. Wang X, Li Q, Li C, et al. Reliability assessment of the fault diagnosis methodologies for transformers and a new diagnostic scheme based on fault info integration. *IEEE T Dielect El In* 2013; 20(6): 2292–2298.
8. Hongbin L, Zhao Q and Yang Z. Reliability modeling of fault tolerant control systems. *Int J Appl Math Comp* 2007; 17(4): 491–504.
9. Ko JM and Ni YQ. Technology developments in structural health monitoring of large-scale bridges. *Eng Struct* 2005; 27(12): 1715–1725.

10. Farrar CR and Worden K. An introduction to structural health monitoring. *Philos T Roy Soc A* 2007; 365(1851): 303–315.
11. Farrar CR, Doebling SW and Nix DA. Vibration-based structural damage identification. *Philos T Roy Soc A* 2001; 359(1778): 131–149.
12. Fritzen CP. Vibration-based structural health monitoring—concepts and applications. *Key Eng Mater* 2005; 293: 3–20.
13. Aldrin JC, Annis C, Sabbagh HA, et al. Best practices for evaluating the capability of nondestructive evaluation (NDE) and structural health monitoring (SHM) techniques for damage characterization. *AIP Conf Proc* 2016; 1706(1): 200002.
14. Stepinski T, Uhl T and Staszewski W (eds). *Advanced structural damage detection: from theory to engineering applications*. Chichester: John Wiley & Sons, 2013.
15. Mendrok K and Uhl T. The application of modal filters for damage detection. *Smart Struct Syst* 2010; 6(2): 115–133.
16. Aldrin JC, Medina EA, Lindgren EA, et al. Case studies for model-assisted probabilistic reliability assessment for structural health monitoring systems. *AIP Conf Proc* 2011; 1335(1): 1589–1596.
17. Mueller I, Janapati V, Banerjee S, et al. On the performance quantification of active sensing SHM systems using model-assisted POD methods. In: *Proceedings of the 8th international workshop on structural health monitoring*, Stanford, CA, 13–15 September 2011, pp. 2417–2428. Stanford, CA: DEStech Publications, Inc.
18. Georgiou GA. PoD curves, their derivation, applications and limitations. *Insight-non-destruct Test Cond Monit* 2007; 49(7): 409–414.
19. Department of Defense. *Department of Defense handbook: nondestructive evaluation system reliability assessment*. MIL-HDBK-1823A, 7 April 2009. Washington, DC: Department of Defense.
20. Ameyaw DA, Rothe S and Söffker D. Adaptation and implementation of probability of detection (POD)-based fault diagnosis in elastic structures through vibration-based SHM approach. In: *9th European workshop on structural health monitoring (EWSHM)*, Manchester, 10–13 July 2018.
21. Ameyaw DA, Rothe S and Söffker D. Probability of detection (POD)-oriented view to fault diagnosis for reliability assessment of FDI approaches. In: *ASME IDETC conference*, Quebec City, QC, Canada, 26–29 August 2018.
22. Schubert KCM, Greenwell BM, DeSimio MP, et al. The probability of detection for structural health monitoring systems: repeated measures data. *Struct Health Monit* 2015; 14(3): 252–264.
23. Moriot J, Quaegebeur N, Le Duff A, et al. A model-based approach for statistical assessment of detection and localization performance of guided wave-based imaging techniques. *Struct Health Monit* 2018; 17(6): 1460–1472.
24. Annis C. Statistical best-practices for building probability of detection (POD) models R package mh.1823, 2017, <http://StatisticalEngineering.com/mh1823/>
25. Gandossi L and Annis C. *Probability of detection curves: statistical best-practices*. ENIQ report 41, 2010. Luxembourg: Office for Official Publications of the European Communities.
26. Knopp JS, Aldrin JC, Lindgren E, et al. Investigation of a model-assisted approach to probability of detection evaluation. *AIP Conf Proc* 2007; 894(1): 1775–1782.
27. Thompson RB, Lindgren E, Swindell P, et al. Recent advances in model-assisted probability of detection. In: *4th European-American workshop on reliability of NDE*, Berlin, 22–26 June 2009.
28. Harding CA, Hugo GR and Bowles SJ. Application of model-assisted POD using a transfer function approach. *AIP Conf Proc* 2009; 1096(1): 1792–1799.

DuEPublico

Duisburg-Essen Publications online

UNIVERSITÄT
DUISBURG
ESSEN

Offen im Denken

ub | universitäts
bibliothek

This text is made available via DuEPublico, the institutional repository of the University of Duisburg-Essen. This version may eventually differ from another version distributed by a commercial publisher.

DOI: 10.1177/1475921719856274

URN: urn:nbn:de:hbz:465-20220329-143411-2

Ameyaw, D. A., Rothe, S., & Söffker, D. (2020). A novel feature-based probability of detection assessment and fusion approach for reliability evaluation of vibration-based diagnosis systems. Structural Health Monitoring, 19(3), 649–660. <https://doi.org/10.1177/1475921719856274>

This publication is with permission of the rights owner freely accessible due to an Alliance licence and a national licence (funded by the DFG, German Research Foundation) respectively.

All rights reserved.